Crystallization of Polymer Melts Under Fast Cooling. II. High-Purity iPP

S. PICCAROLO,* M. SAIU, V. BRUCATO, and G. TITOMANLIO

Dipartimento di Ingegneria Chimica dei Processi e dei Materiali, Università di Palermo, 90128 Palermo, Italy

SYNOPSIS

Samples of a high-purity isotactic polypropylene (iPP) were quenched from the melt so as to monitor cooling history. A continuous variation of morphology and crystal structure was obtained with cooling rate. This is discussed in relation to sample thermal history evidencing that cooling history relevant to quenched samples is in the neighborhood of 90°C. In particular the samples are essentially mesomorphic when at this temperature cooling rates larger than 80°C/s were adopted, while below a few tens of °C/s only α-monocline form is obtained. Densities of quenched samples were compared with predictions of an isokinetic extrapolation of Avrami model of polymer crystallization kinetics.

INTRODUCTION

A detailed quantitative knowledge of crystallization kinetics and modes is still to be achieved for all thermo-plastic polymers in spite of the large amount of work devoted to this subject. This is in relation to the obvious difficulties of quantitative analysis for those polymers that at some temperature can crystallize significantly in times of the order of a tenth of a second; in these cases, indeed, a reliable isothermal crystallization test cannot be performed in a standard calorimeter, which cannot exceed a cooling rate of a few degrees per second, since crystallization takes place while the sample reaches the test temperature. Furthermore, for the same reason, information obtained from calorimetric cooling ramps is poor, as equilibrium crystallinity is closely approached for a wide temperature interval, and data with regard to equilibrium crystallization rather than to kinetics are collected. On the other hand cooling histories from the melt experienced by the material in usual polymer processing operations can well be much higher than those of a standard calorimeter. A light depolarization method[1-3] was expressly developed in order to follow crystallization during isotherms at large degrees of supercooling. The method proved much more versatile than other procedures adopted to study crystallization kinetics, however, cooling histories to test temperatures were not measured.

With reference to isotactic polypropylene (iPP) it is known that[4,5] crystallization toward α-crystalline structure is preferred at high temperature whereas a mesomorphic highly disordered phase[6-9] is mainly obtained at lower temperatures; furthermore various quenching techniques[10-13] have been developed. These were adopted to study structural transitions taking place in highly quenched samples by the effect of subsequent heating. No crystallization kinetic data are, however, available at such high cooling rates.

The study of crystallization of iPP under high cooling rates remains thus of technological interest, and a contribution to this matter is given in this work by analyzing the structure of thin polymer samples quenched so as to monitor cooling history from the melt.

EXPERIMENTAL

The material studied was an injection moulding grade iPP kindly supplied by Himont. In relation to the small ash residue (15–17 ppm), it can be considered high purity; other characteristics are: melt flow index (MFI) 4.3 g/10 min at 230°C, M_n

* To whom correspondence should be addressed.

Journal of Applied Polymer Science, Vol. 46, 625–634 (1992)
 CCC 0021-8995/92/040625-10

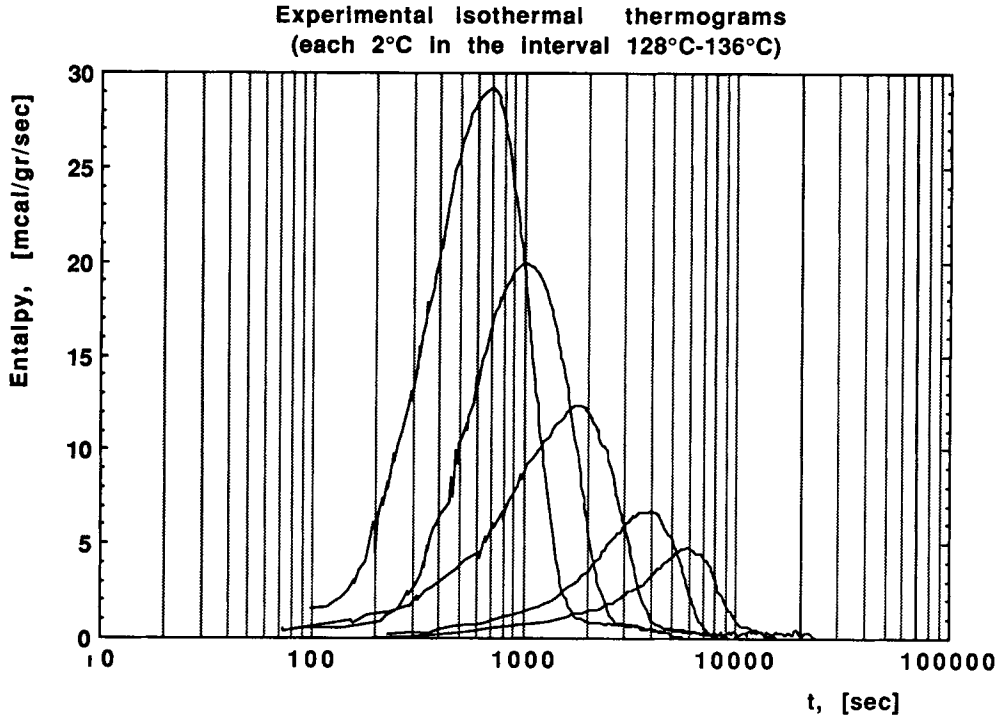

Figure 1 Isothermal thermograms each 2°C in the interval 128–136°C.

= 79,300, M_w = 476,000. Some crystallization isotherms were performed every 2°C in the temperature interval 128–136°C using a DSC4 Perkin-Elmer instrument. The samples were held at 230°C for 30 min before cooling them to the temperature of the isotherm. The results, reported in Figure 1, show that a reliable calorimetric test cannot be performed at temperatures lower than 120°C since time to

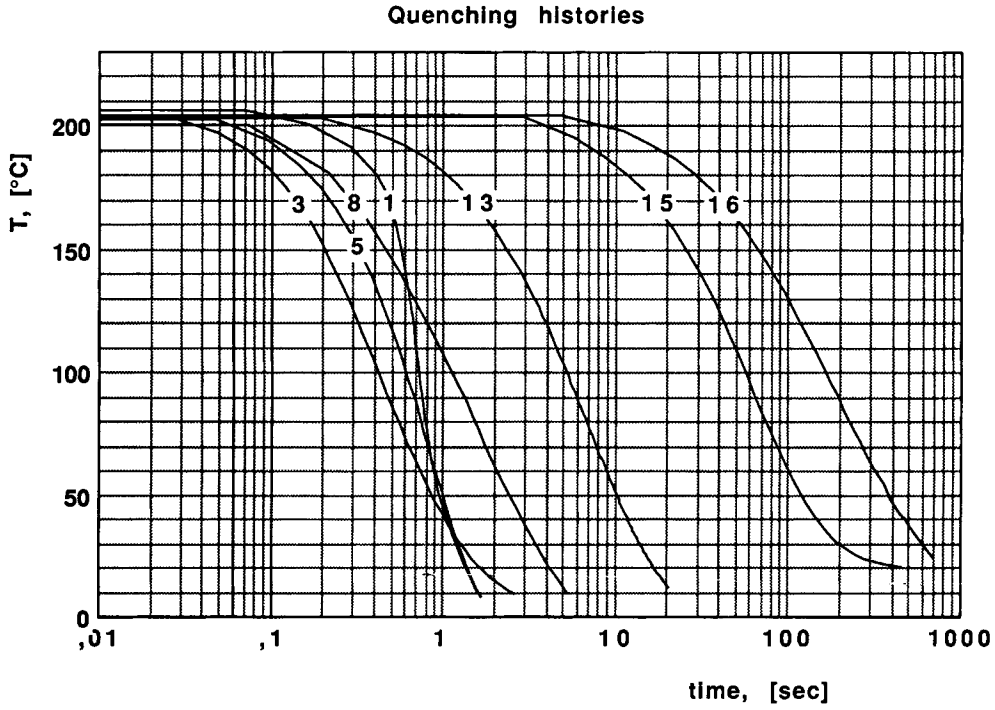

Figure 2 Samples of cooling histories.

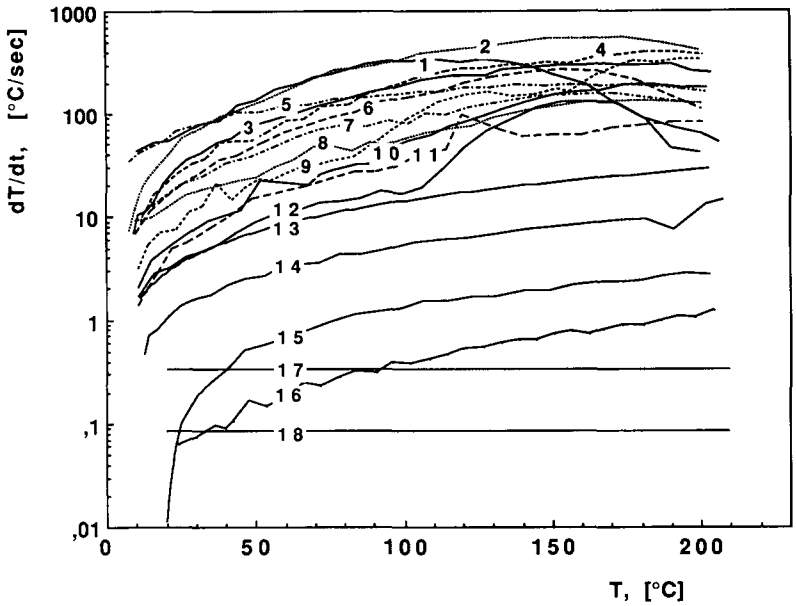

Figure 3 Cooling rate vs. temperature in quenching procedures, sample number refers to Table I.

reach this figure (at a maximum cooling rate of 100°C/min) would become of the order of the time for maximum crystallization rate.

In order to gain information regarding the crystallization kinetics at lower temperatures, 50–100 μm thin samples of the material were packed in a folded 20-μm aluminum foil and assembled in suitable copper dies whose total thickness ranged in the interval 1.5–5 mm, then the die was quenched in a liquid cool bath while the die temperature was recorded according to a procedure previously described;[14] sample and die thickness were kept so as to ensure values of Biot numbers smaller than 0.05, thus assuring sufficient temperature homogeneity within the sample.

Typical thermal histories obtained with this pro-

Table I Density, Relevant Cooling Rate at 90°C and Experimental and Calculated Crystallinities

Sample	Quench No.	Density (g/cm^3)	T, @ 90°C (K/s)	X_f Exp.	X_f calc. n = 0, 25
1	Q45	0.8835	311	24.8	24.2
2	Q34	0.8838	297	25.2	24.1
3	Q33	0.8842	165	25.7	27.1
4	Q35	0.8846	162	26	27.4
5	Q37	0.8846	146	26	27.3
6	Q44	0.8856	123	27.5	28.5
7	Q49	0.8865	78	28.7	30
8	Q50	0.8898	51	32.9	32.6
9	Q36	0.8927	51	36.6	36
10	Q40	0.8923	36	36	34.5
11	Q46	0.8923	27	36	36
12	Q43	0.8980	16.8	43.3	38.3
13	Q51	0.8989	12.7	44.5	39.4
14	Q38	0.8989	4.6	44.5	44.3
15	Q39	0.9020	1.19	48.5	49.5
16	Q52	0.9034	0.28	50.2	52.6
17	Q53	0.9038	0.33	50.7	52.4
18	Q54	0.9067	0.0833	54.3	54.2

cedure are reported in Figure 2 as temperature versus time and the time differential of temperature is plotted versus temperature in Figure 3. Samples 17 and 18 were obtained by the same calorimeter adopted for the isothermal tests operated under constant cooling rate. All the samples were held at 230°C for 30 min before being subjected to the cooling procedures.

The solid samples obtained were maintained at −20°C before being subjected to density measurements, Wide-angle X-ray diffraction (WAXD), and polarized optical transmission microscopy.

Sample densities were determined by a liquid gradient column prepared with distilled water and ethanol. The sample densities determinations are reported in Table I.

WAXD scans were performed in the 2θ interval from 6° to 45° under Ni-filtered CuKα radiation with a computer-assisted goniometer accomplishing an optimized step scanning of 0.05°–0.2°, depending on peak height and derivative, with a count time of 60 s. The diffractograms are reported in Figure 4.

Figure 5 shows some transmission optical micrographs obtained under polarized light on samples etched with a procedure recently developed for polyolefins.[15,16] The micrographs are ordered from left to right and from top to bottom according to the values of cooling rate $\dot{T}_{90}$ at 90°C. This cooling rate is also reported in Table I and was found a suitable macroscopic measure of quenching effectiveness for this material.

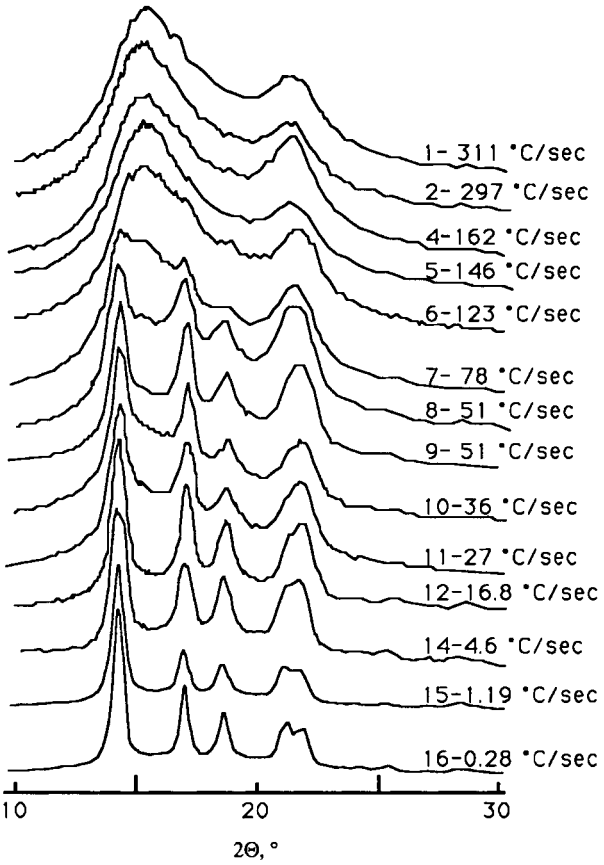

Figure 4 WAXD patterns, sample number refers to Table I.

DISCUSSION

Thermal histories experienced by the samples during quenching procedures explore a wide range of cooling rates, reaching values as high as 300°C/s. Several crossings are observed among the cooling histories of Figure 3, however, densities of quenched samples increase monotonously toward a plateau (Table I) when plotted against cooling rate in the neighborhood of 90°C.

The relation between quenching effectiveness and $\dot{T}_{90}$ is further proved in Figure 4, where X-ray diffractograms are reported. In particular the X-ray patterns reported in Figure 4 show a continuous increase of perfection of crystalline entities as the cooling rate at 90°C, $\dot{T}_{90}$, decreases:

1. Samples from 1 to 5 (down to $\dot{T}_{90}$ = 146°C/s) are mesomorphic, and the secondary peak at 2θ = 21.5° sharpens as $\dot{T}_{90}$ decreases, thus showing an improvement of the long-range order.
2. A transition from mesomorphic to α-monocline structure is observed from the diffractograms of samples 6 and 7 ($\dot{T}_{90}$ = 120 and 78°C/s, respectively); indeed the stronger peak at 2θ = 15° shifts to lower angles characteristic of the α (110) reflection at 2θ = 14.08° and the other reflections (040) and (120) start to be evidenced at 2θ = 16.95° and 2θ = 18.5°, respectively.
3. Samples from 8 to 11 show a continuous sharpening of all the α peaks, but the ones related to reflections (111) and (131) at 2θ = 21.2° coupled with (041) at 2θ = 21.85° takes place.
4. Finally for samples 12 to 16 the latter reflections also become more clearly resolved.

Some micrographs of the quenched samples are reported in Figure 5. These are in line with previous (WAXD and density) findings and confirm the mo-

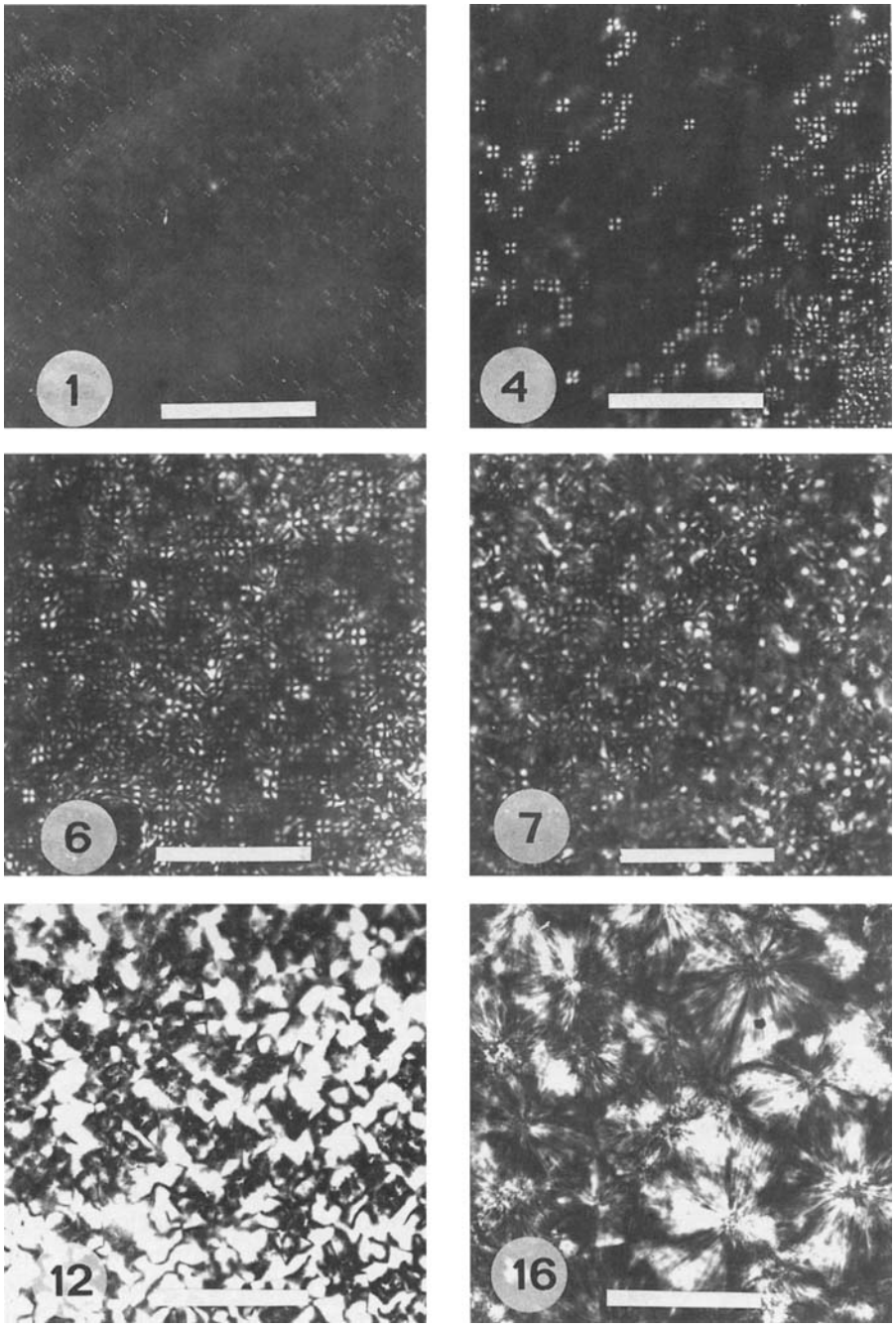

Figure 5 Optical polarized micrographs, sample number refers to Table I. Scale bar is 100 μm.

notonous change of structure with cooling rate, $\dot{T}_{90}$. In particular, some isolated spherulites are observed, dispersed in a weakly birefringent medium, in the micrographs of samples 1 and 4. Sample 6 contains spherulites having dimensions and appearance similar to those found in sample 4, although the field of view is almost completely filled many of them appear isolated. The spherulites observed in samples 7–11 appear to fill completely the field of view and, being smaller than sample thickness, interact with each other's extinction pattern. Impinging spherulites, which are already observed in sample 6, become predominant on lowering cooling rate. Spherulites of samples 1–11 are negatively birefringent with a

well-developed maltese cross clearly evident in sample 4 but already recognizable also in sample 1.

The structure most commonly encountered in melt solidified iPP, composed of mixed spherulites, was observed with samples 12–16, i.e., for cooling rates $\dot{T}_{90}$ smaller than 17°C/s.

On decreasing cooling rate an increase of spherulites dimensions is registered with a monotonous but peculiar dependence on cooling rate. Indeed spherulite sizes of about 1, 10, 20, 40, and 100 μm were observed with samples 1, 4, 6–12, 15, and 16, respectively. An increase in spherulite dimensions is therefore first observed on decreasing cooling rate down to $\dot{T}_{90}$ = 120°C/s, in the range of cooling rates from about 120 to 17°C/s they remain essentially constant and start to increase again below 17°C/s.

Samples 1–4 closely resemble each other as far as spherulite density is concerned, this density becomes significantly higher for sample 6, i.e., on lowering the characteristic cooling rate, $\dot{T}_{90}$, in a narrow range (from 160 to 120°C/s) and becomes still higher for sample 7. Furthermore it certainly decreases when size of impinging spherulite grows and the competition for melt consumption by spherulite growth takes place. A maximum of spherulite density is therefore observed for a $\dot{T}_{90}$ of a few tens of °C/s. An inverse behavior can presumably be attributed to primary nucleation density.

As shown by WAXD the mesomorphic and the α-monocline structure are of comparable amount in sample 7. The problem arises in trying to reconcile the WAXD evidence with the almost complete spherulitic morphology, no spherulitic texture was indeed observed in highly quenched mesomorphic iPP, only very small nodules in the 10–35 nm range have been previously[11,12] observed that would coarsen on annealing above about 70°C. The coexistence of the two phases can only be explained if the mesomorphic phase is intermixed with α-monocline crystals constituting the spherulites. Similar observations can be made on samples 8–10 although a significant contribution to their WAXD spectrum broadening has also to be ascribed to the broadening of the α peaks due to the high level of disorder and size distribution of the α-crystalline structure formed at these cooling rates.

This discussion was developed taking $\dot{T}_{90}$ as a macroscopic measure of "quenching effectiveness." Obviously this has to be taken only as a first approximation and in any case needs some specifications.

If cooling rate is small enough to let samples crystallize at high temperature (larger than 90°C), quenching effectiveness cannot be regulated by $\dot{T}_{90}$: therefore the portion of cooling history regulating quenching effectiveness has to be dependent on this cooling rate, at least to some extent.

In order to gain some insight regarding this feature, let us consider cooling histories reported in Figure 3. In this figure there are crossings between cooling histories of sample pairs 17 and 16, 9 and 8, and 5 and 4. In particular samples 17, 8, and 5 underwent a faster cooling rate below crossing temperatures in the neighborhood of 90, 90, and 85°C, respectively. Both densities reported in Table I and mainly WAXD scans of Figure 4 identify samples 16, 8, and 5 as more effectively quenched than samples 17, 9, and 4, respectively. One can thus conclude that quenching effectiveness is determined by thermal history: above 90°C for cooling rates of the order of that experienced by samples 16 and 17 (i.e., about 0.3°C/s), below 90°C for cooling rates of the order of that experienced by samples 8 and 9 (i.e., about 50°C/s), below 85°C for cooling rates of the order of that experienced by samples 4 and 5 (i.e., about 150°C/s).

All these observations can be summarized as follows: when cooling rate is small, the material crystallizes toward α form; crystallization toward mesomorphic aggregates remains thus inhibited and the cooling rate above 90°C regulates density and crystallinity; at a cooling rate of some tenths per second negatively birefringent spherulites start to form and spherulite density shows a maximum; at 50°C/s α form remains dominant and quenching effectiveness is regulated by cooling rate below 90°C. When cooling rate is of the order of 70°C/s, only a small amount of α-crystalline form is revealed, and crystallization to the disordered mesomorphic form is preferred (at lower temperature). The spherulites produced under these conditions are sparse and do not impinge against each other. The mesomorphic phase becomes dominant when cooling rate is of the order of 150°C/s or above; under these conditions the relevant cooling rate is at a temperature below 85°C and few isolated spherulites are observed.

ANALYSIS OF RESULTS

A detailed mathematical description of the crystallization phenomenon taking place during quenching of iPP should consider that there are at least two crystallization processes: a monocline phase forms at low cooling rates and a mesomorphic phase characterized by a high degree of disorder forms at higher

cooling rates and lower temperature. The two processes are competitive. After X-ray deconvolution, one could attempt to identify a detailed kinetic description and face the problem of interaction between them.

Only the possibility of describing the overall crystallinity by a single equation was analyzed in this work. To this purpose a single crystallinity index was drawn from density measurements. It was obtained on the basis of amorphous and crystalline densities at 25°C, 0.8562 and 0.9346 g/cm^3, respectively, of α monocline form,[17] thus obtaining an α equivalent crystallinity index reported in Table I. These results are compared here with the predictions of a nonisothermal isokinetic formulation of Avrami[18–20] and Evans[21] model for crystallization kinetics. This formulation accounts for temperature dependence of equilibrium crystallinity as suggested by Malkin et al.[22,23] and can be summarised as follows:

$$\frac{dX}{dt} = [X_{eq}(T) - X] \times n \ln 2 \left[\int_0^t K(T)\, ds\right]^{n-1} K(T) \quad (1)$$

where $K(T)$ is the kinetic constant given by

$$K(T) = K_c \exp\left[-\frac{4 \ln 2 (T - T_{max})^2}{D^2}\right] \quad (2)$$

The following equation was adopted for X_{eq}:

$$X_{eq} = \xi \frac{T_m - T}{T_1 - T} \quad (3)$$

where ξ, T_m, T_1 are material constants and $X_{eq} = 0$ for $T > T_m$ was adopted for X_{eq}.

In a previous study,[14] it was shown that, apart from a time scale factor related to the constants of Eq. (2), the relation between final crystallinity of the solid after a quenching and cooling rate depends only upon the Avrami index n, if X_{eq} is constant and also if it grows smoothly as temperature decreases in the zone when $K(T)$ has the maximum.

The comparison between the experimental equivalent crystallinity and model predictions evaluated by means of Eqs. (1)–(3) is shown in Figure 6 for the samples whose cooling histories are reported in Figure 3. The constants of Eq. (3) were identified as

$$\xi = 0.587 \qquad T_m = 436 \text{ K} \qquad T_1 = 440.8 \text{ K}$$

on the basis of high-temperature calorimetric tests; they assure a very smooth increase of X_{eq} on decreasing temperature after a sharp growth at about 150°C.

The constants of Eq. (2) were best fitted on both final crystallinity of all samples that experienced different thermal histories and high-temperature values of crystallization half-times of isotherms, t_h.

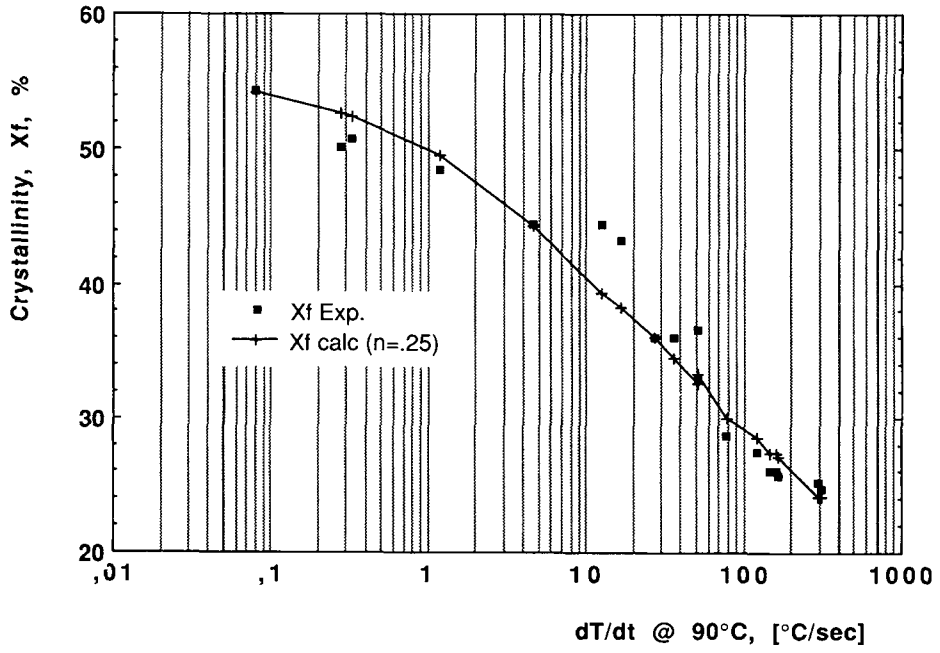

Figure 6 Solid crystallinity X_f vs. cooling rate at 90°C, comparison between model predictions and data.

The data of final crystallinity identify both the value of n and the product K_cD. In particular the product K_cD is identified as 141 K/s; and a very small value, $n = 0.25$, is required for n. Such a small value of n is in relation to the very slow increase of the experimental final crystallinity, which approximately doubles as cooling rate decreases by more than three orders of magnitude.

Furthermore, high-temperature values of K_c drawn from crystallization half-times of isotherms, t_h, give rise to another constraint. One degree of freedom is then left in the identification of the parameters of Eq. (2) as for each value of D, K_c is determined as $K_c = 141/D$ and T_{max} remains determined by the high-temperature values of K_c. An upper bound for K_c versus T curve width, D, is however identified by the observation that in the neighborhood of ambient temperature crystallinity does not change significantly with time.

Figure 7 reports both the $1/t_h$ values identified by means of isotherms and the whole curve $K(T)$ calculated on the basis of the above-mentioned upper bound for D and in particular with

$$T_{max} = 362 \text{ K} \qquad K_c = 6 \text{ s}^{-1} \qquad D = 23.5 \text{ K}$$

The data of $1/t_h$ suggest a slope smaller than the one shown by the curve. Since the curve would attain a smaller slope in the temperature range of the $1/t_h$ data only if larger values of D would be adopted, the curve reported in Figure 7, that is evaluated on the basis of the upper bound for D, of the product K_cD and of the $1/t_h$ data, can be considered as a best fitting.

Figure 6 reports experimental as well as calculated final crystallinity of the samples versus $\dot{T}_{90}$; letter points are evaluated on the basis of the experimental cooling histories, which determine a slightly jagged curve since $\dot{T}_{90}$ does not completely identify the related thermal history.

The comparison shown in this figure is satisfactory; on the other hand it has to be pointed out that, with values of n smaller than 1, predictions of Avrami model for an isothermal test do not give a maximum for the crystallization rate versus time. However, it must be remembered that this is a simple attempt of describing the crystallization kinetic by

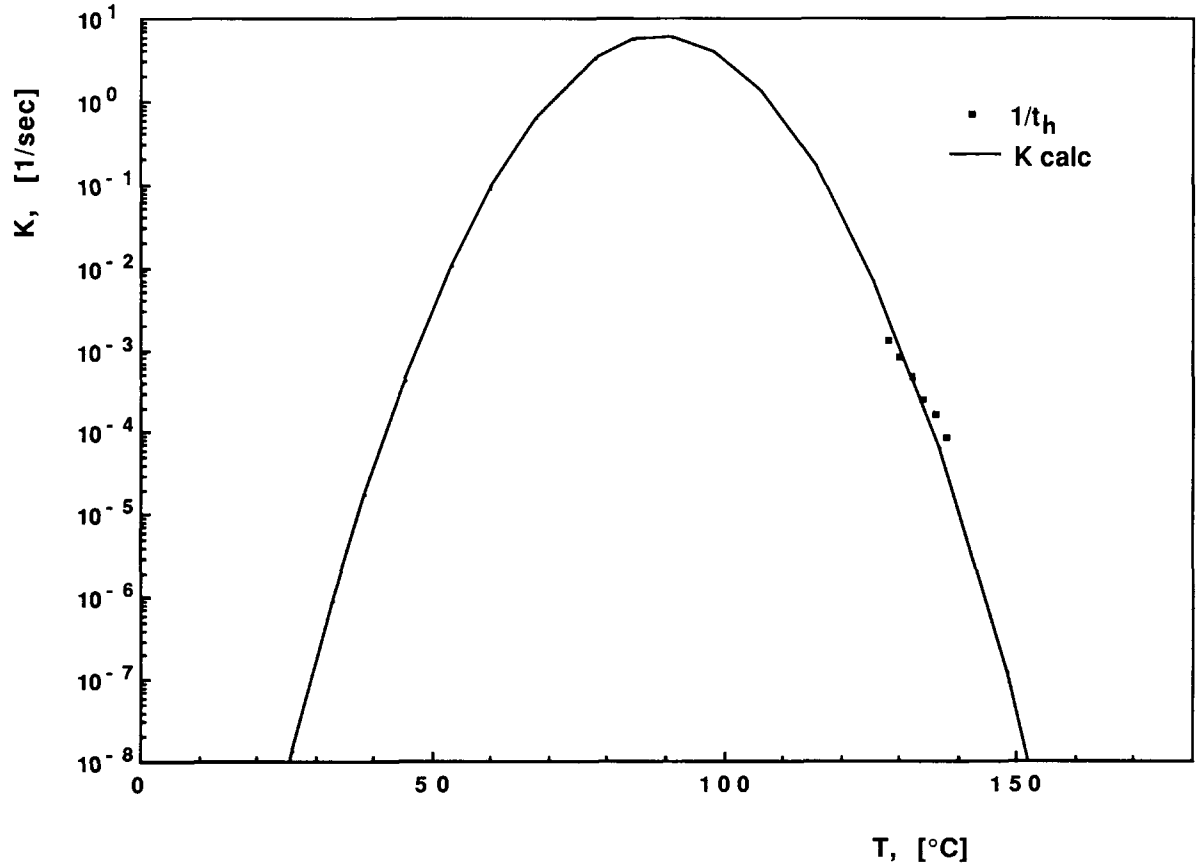

Figure 7 $K(T)$ vs. T, dots are reciprocal of isothermal crystallization half time, t_h.

a single equation while there is experimental evidence of the formation of at least two crystalline phases. As a consequence, only a partial description of the data is not surprising and in any case the parameters of Eqs. (1) and (2) cannot have any physical meaning. The possibility of adopting a parallel of two kinetic equations to describe the experimental density (crystallinity) behavior has to be considered.

CONCLUSIONS

The samples obtained by the quenching procedure adopted in this work cover a wide range of cooling rates giving rise to a monotonous variation of structure "perfection" with cooling rate.

Density, WAXD, and microscopic observations show that the thermal history segment relevant to quenching of iPP is in the neighborhood of 90°C.

When cooling rate $\dot{T}_{90}$ is larger than about 80°C/s, the mesomorphic phase dominates the conversion of melt to solid with some few isolated negatively birefringent spherulites. For cooling rates smaller than a few tens of °C/s the mesomorphic phase is replaced in the quenched samples by the α-monoclinic phase. Between these values of cooling rate, mesomorphic and α-monoclinic forms compete in the crystallization process. Mixed spherulites are first detected at a cooling rate of a few tens of °C/s with dimensions of about 20 μm, their size increasing markedly below a $\dot{T}_{90}$ of about 1°C/s.

A nonisothermal form of Avrami model was tried to describe the crystallization kinetics. It was found able to give a macroscopic description of final crystallinity of quenched samples, but only with a very small value of the exponent n, which is not consistent with the results of high-temperature isothermal calorimetric tests. As crystallization takes place toward both monoclinic and the more disordered mesomorphic forms, the failing of the attempt to describe both densities of quenched samples and high-temperature isothermal calorimeter results by a single kinetic equation is not surprising. The success of such an attempt would have not given a description of reality but rather a fortunate possibility to macroscopically describe density changes that take place in polymer processing.

The next attempt should be a closer description of the observed phenomena, in particular the experimental observations suggest a parallel of two kinetic equations to describe α and mesomorphic crystallization. If the Avrami model holds for both processes, α crystallization (which takes place at larger temperature) could be related to a higher value of Avrami index n as suggested by isothermal calorimetric results, a lower n value could be related to low-temperature mesomorphic crystallization, which could be diffusion controlled. The experimental information of this analysis could be found in the deconvolution of WAXD spectra of samples of Figure 3, which are characterized as far as temperature history.

LIST OF SYMBOLS

D	material constant, see Eq. (2) (K)
iPP	isotactic polypropylene
$K(T)$	kinetic constant as function of temperature (s^{-1})
K_c	maximum value of kinetic constant (s^{-1})
n	Avrami exponent, see Eq. (1), dimensionless
M_n	number-average molecular weight
M_w	weight-average molecular weight
MFI	melt flow index
t	time (s)
t_h	half-times of isothermal crystallization (s)
T	temperature (K)
T_m	experimental constant, see Eq. (3) (K)
T_1	experimental constant, see Eq. (3) (K)
T_{max}	temperature of maximum of $K(T)$ (K)
$\dot{T}_{90}$	cooling rate at 90°C (K/s)
X	crystallinity index, dimensionless
X_{eq}	equilibrium crystallinity, dimensionless
X_f	crystallinity after quenching, dimensionless

Greek Symbols

α,	crystalline phase
ξ,	experimental constant, see Eq. (3), dimensionless

REFERENCES

1. J. H. Magill, *Polymer*, **2**, 221 (1961).
2. J. H. Magill, *Polymer*, **3**, 35 (1962).
3. J. H. Magill, *Polymer*, **3**, 655 (1962).
4. D. R. Morrow, *J. Macromol. Sci., Phys.*, **B3**, 53 (1969).

5. A. Turner Jones, J. M. Aizlewood, and D. R. Beckett, *Makomol. Chem.*, **75,** 134 (1964).
6. P. G. Schmidt, *J. Pol. Sci.*, **A1,** 2317 (1963).
7. P. J. Hendra, J. Vile, H. A. Willis, V. Zichy, and M. E. A. Cudby, *Polymer,* **25,** 785 (1984).
8. M. Glotin, R. R. Rahalkar, P. J. Hendra, M. E. A. Cudby, and H. A. Willis, *Polymer,* **22,** 731 (1981).
9. P. Corradini, V. Petraccone, C. DeRosa, and G. Guerra, *Macromolecules,* **19,** 2699 (1986).
10. D. M. Gezovich and P. H. Geil, *Polym. Eng. Sci.,* **8,** 202 (1968).
11. C. C. Hsu and P. H. Geil, *J. Appl. Pol. Sci.,* **24,** 2379 (1986).
12. D. T. Grubb and D. Y. Yoon, *Polymer Comm.,* **27,** 84 (1986).
13. R. Zannetti, G. Celotti, A. Fichera, and R. Francesconi, *Makromol. Chem.,* **128,** 137 (1969).
14. V. M. B. Brucato, G. Crippa, S. Piccarolo, and G. Titomanlio, *Polym. Eng. Sci.,* to appear.
15. R. H. Olley and D. C. Basset, *Polymer,* **23,** 1707 (1982).
16. F. Rybnikar, *J. Appl. Pol. Sci.,* **30,** 1949 (1985).
17. F. Danusso, G. Moraglio, W. Ghiglia, L. Motta, and G. Talamini, *La Chim. l'Industria,* **41,** 749 (1959).
18. M. Avrami, *J. Chem. Phys.,* **7,** 1103 (1939).
19. M. Avrami, *J. Chem. Phys.,* **8,** 212 (1940).
20. M. Avrami, *J. Chem. Phys.,* **9,** 177 (1941).
21. U. R. Evans, *Trans. Faraday Soc.,* **41,** 365 (1945).
22. A. Y. A. Malkin, V. P. Beghishev, I. A. Keapin, and S. A. Bolgov, *Polym. Eng. Sci.,* **24,** 1396 (1984).
23. A. Y. A. Malkin, V. P. Beghishev, I. A. Keapin, and Z. S. Andrianova, *Polym. Eng. Sci.,* **24,** 1402 (1984).

Received November 4, 1991
Accepted December 10, 1991